Vibration Anomaly Detection by Clustering in Unmanned Aerial Vehicles.

Portia Banerjee*
KBR, NASA Ames Research Center, Moffett Field, CA 94035.

Rajeev Ghimire†
KBR, NASA Ames Research Center, Moffett Field, CA 94035

Elizabeth Hale‡
NASA Ames Research Center, Moffett Field, CA 94035

One of the critical factors affecting flight safety of unmanned aerial vehicles (UAVs) is the amount of vibration they are exposed to during a flight. On one hand, external causes such as wind gusts and turbulences or internal vehicle-centric faults such as incorrect sensor mounting or propeller imbalances can cause high vibrations in UAVs. On the other hand, high vibration itself may induce noise in the onboard miniature sensors of the UAV such as its accelerometers, gyroscopes and GPS that can lead to uncertain state estimation causing the multi-rotor to drift from its desired position or even result in loss-of-control. Hence, it is important to monitor the vibration levels during a UAV flight. This paper specifically looks into vibrations recorded by the autopilot system of a multi-rotor in presence of varying magnitudes of wind. Using data from experimental flights conducted at two separate flight test regions under varying wind conditions, we aim to classify between a nominal and anomalous vibration level for small UAV systems. Further, we analyse other parameters of interest that affect vibrations in UAVs such as UAV air speed and any propeller imbalance signatures. Analysis results from experimental flights demonstrate the effect of wind on vibration magnitude in unmanned aircrafts.

I. Motivation and Related Work

Unmanned Aerial Vehicles (UAVs) are becoming increasingly common in several applications, including aerial photography, surveillance, package delivery, and precision agriculture. While smaller aircrafts offer numerous benefits, unique challenges arise with UAV flight safety especially due to small size of these vehicles in combination with turbulence arising in the low altitude airspace. Larger manned aircrafts typically incorporate numerous redundancies in their monitoring and control systems to ensure safety, but UAVs are restricted by their size and weight. Therefore, it is critical to develop effective health monitoring systems for UAVs that can ensure continued and risk-averse operation.

Fault detection and diagnosis (FDD) is widely studied and applied to several components in UAVs to assess the state of the vehicle and determine need for either early flight termination or vehicle maintenance or trajectory re-planning. Under development of advanced in-time safety assurance tools that can monitor, assess and mitigate risks for UAV operations [1], several efforts have been made to investigate FDD methods on UAV powertrain components including propellers and motors [2, 3]. Over the last several years, analysis of vibration signals for FDD in UAVs, has become an increasingly popular area of study [4, 5]. Applications of such analysis can range from overall flight anomaly detection [6], and diagnosing or predicting specific failure modes, such as FDD of propeller damage and friction [4, 7] or issues with excessive payload [5], to simply determining the optimal location for instrument placement to minimize the effects of nominal vibrations [8]. Frequency analysis is a common approach to understand vibration signals originating from rotating parts, such as the motors and propellers in an aircraft, especially for fault analysis, as it can reveal features in the frequency domain that arise as a result of changes in the usual periodic behavior of these components [5]. There are a wide variety of approaches to frequency analysis, including the classical Fourier transform as well as the newer wavelet decomposition and variations on each of these in an effort to resolve issues with loss of time information and cross-term interference [9–11]. However, one of the key challenges that we face in a typical small UAVs is low data sampling rate

*Research Engineer, Intelligent Systems Division, portia.banerjee@nasa.gov, AIAA Member, Corresponding author.
†Research Engineer, Intelligent Systems Division, rajeev.ghimire@nasa.gov, AIAA Member.
‡NASA Pathways Intern, Intelligent Systems Division, elizabeth.hale@nasa.gov, AIAA Member.

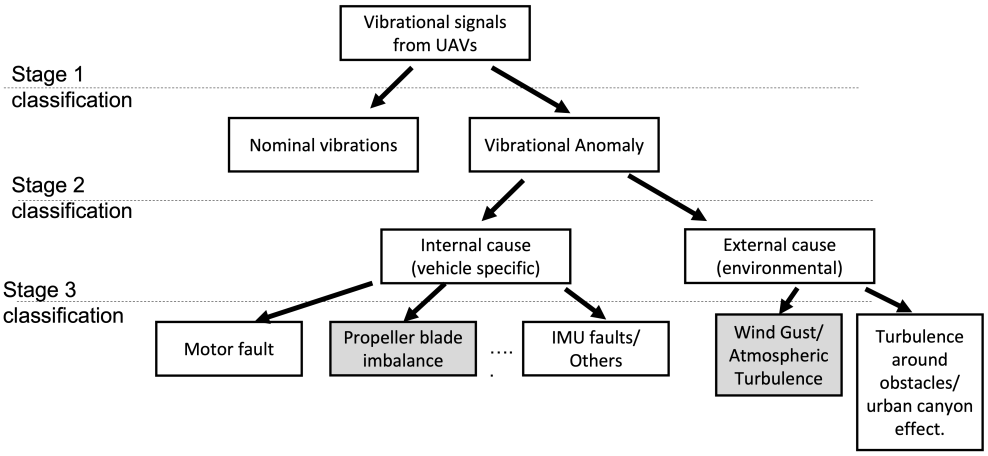

Fig. 1 Vibrational Anomaly Detection and classification for a UAV- concept flowchart.

from on-board autopilot systems which limits our capability of obtaining key frequency domain features from the UAV vibration data that can reasonably detect any anomaly. As a result, in this study we resort to time-series analysis and data-mining methods to extract distinct signatures indicative of anomalies in UAV flights.

When looking at a vibration signal to extract information on vehicle health, a three stage classification system can be helpful, as shown in Figure 1. Upon measuring the vibration signal, the first stage of classification would be to determine if the vibration is a nominal vibration resulting from expected sources in the aircraft such as its rotating components, or if it is an anomaly that affects flight safety. If the vibration is classified as an anomaly, the second stage is to determine if the cause is internal or external to the aircraft. When the anomaly is due to a fault within the aircraft, the third and final stage would be to isolate the anomaly source such as motor failure, propeller imbalances or IMU degradation. However, before attempting to diagnose a fault within the aircraft, causes external to the system should be eliminated. Therefore, of particular interest in this study is determining when anomalies are due to external factors, specifically wind. Particularly for low-altitude airspace where typical small and mid-size UAVs are planned to operate, atmospheric turbulence and wind gusts are a major source of disruptions to its planned path causing trajectory deviations [12] and may lead to higher than expected vibration levels. An additional interest to identify the source of vibration anomalies is that decision making post anomaly detection depends on the source. For example, if a UAV is operated on a wildfire monitoring zone with high wind and high temperature environment and it experiences vibrations caused due to the external factors, it needs to be re-routed or re-planned accordingly. On the other hand, if vibrations arise from a vehicle-centric fault, the UAV operation may need to be terminated, either taken out for repair or replacement. Hence it is important to study the effect of both external and internal factors on UAV vibrations. In this paper, we focus on studying the effect of wind on vibrations measured by on-board sensors on the UAV. In section II, different sources of vibration anomalies and their effect on UAV flight safety are reported based on the findings from related studies in literature. Section III presents the K-means clustering algorithm that is implemented in this study to group UAV data based on vibration related parameters. In section IV, specific flight data obtained from UAV flight experiments conducted at varying wind conditions are analysed. Finally, high dependence of vibration levels in UAVs on wind gust and vehicle factors such as propeller imbalance are identified from the results with the study being concluded in section V.

II. Failure Mode and Effect Analysis of Vibrations in UAVs

Failure mode and effects analysis (FMEA) is a systematic approach widely used in system health management and reliability studies in order to identify possible failure sources, their causes, criticality aspects, and impact on the overall system. It helps prioritize fault handling in the event of failures. It is important to identify failures in UAVs and their root causes that are related to vibration as those may have direct and indirect relation to the UAV operational safety. Internal subsystems in UAVs, such as unbalanced propellers or propeller damage, motor bearing issues, and poor motor control (less damping) can cause vibrations. On the other hand, environmental disturbances such as high wind/wind-gusts can also cause vibrations in UAVs during its flight. Hang et al. reported that along with the rotating parts and equipment malfunction, different types of wind (turbulent flow, wind shear, propeller vortex, etc.) may cause

abnormal vibration in UAVS [13]. The wind interaction with UAV body and propeller changes due to wind turbulence, wind gusts, and other environmental factors such as terrain, altitude, temperature, etc., have also been reported in [14]. Other causes such as insufficient damping caused by possible sensor malfunction may result in reduced capability the UAV to control the vibrations [13]. Moreover, sustained vibrations can cause other components to fail in the UAV systems. The objective of this FMEA study is to recognize vibration-related failures, their root causes, and effects to aid in understanding the failure origination, detection, and diagnostic process. There are different FMEA-related studies for UAV system reported in the literature [6, 7, 15, 16] focusing on various components of a UAV system. Table 1, summarizes FMEA of UAVs that are directly or indirectly related to vibrations. It has columns a) component, b) failure mode, c) root cause, d) effects, e) relation to vibration, f) likelihood and e) severity. It should be noted that vibration in a UAV itself can either be an effect of another source or a cause to another failure in the system (or sometimes both), as indicated in the'relation to vibration' column. There are four different category labels in this column of the FMEA table. A direct effect means that vibration is the failure mode directly leads to vibration anomalies in the UAV whereas an indirect effect means the failure mode leads to another characteristic change in the UAV which in turn leads to faulty vibrations. Similarly meaning is attached to direct and indirect cause. Moreover, some failure modes may result from external vibration (as the cause) and the failure mode effect can be internal vibration (see row 1) .The likelihood of a failure and its severity are classified into three levels: low (L), medium (M) or high (H) [16].

Table 1 FMEA of vibration anomaly in UAV systems

SN	Component	Failure Mode	Root Cause	Effects	Relation to vibration	Likelihood	Severity
1.	Airframe	Main body or Wings -structural	Collision/ bad landing /external vibrations	Altered aerodynamics/ loss of functionalities	Direct cause and effect	L	M
2.	Motor	Bearing	Lubrication/hard failure	Motor rotation, thrust, loss of control	Indirect effect	M	H
3.	Motor	Unbalanced rotor	Rotor damage/Shaft misalignment	Increased vibration/ motor rotation	Direct effect	L	M
4.	Motor	Coil Short circuit/windings	Propeller unbalanced vibrations	Loss of thrust/incorrect motor speed, loss of control	Direct cause	L	M
5.	Propeller blades	Structural/ cracking	Collision/ bad-landing/ Imbalance/ Vibration	Loss of thrust/ loss of control	Direct cause	L	M
6.	Connecting cables/wires	Disconnection from sources to receiver/ load	Severed wire/ excessive vibration	Loss of power, comms., data, vehicle controllability, vehicle failure	Direct cause	H	H
7.	Sensor fault (IMU)	malfunction/ power-loss	internal/ external vibration, physical damage, temperature variation	Incorrect measurements, data issues, control issues, loss of thrust	Direct/indirect cause	M	H

III. k-means Clustering of Vibration Data

Based on the above FMEA, we determined that high vibrations may be caused due to multiple reasons and not all high vibration necessarily indicates a faulty UAV system. In order to classify nominal versus anomalous vibrations in

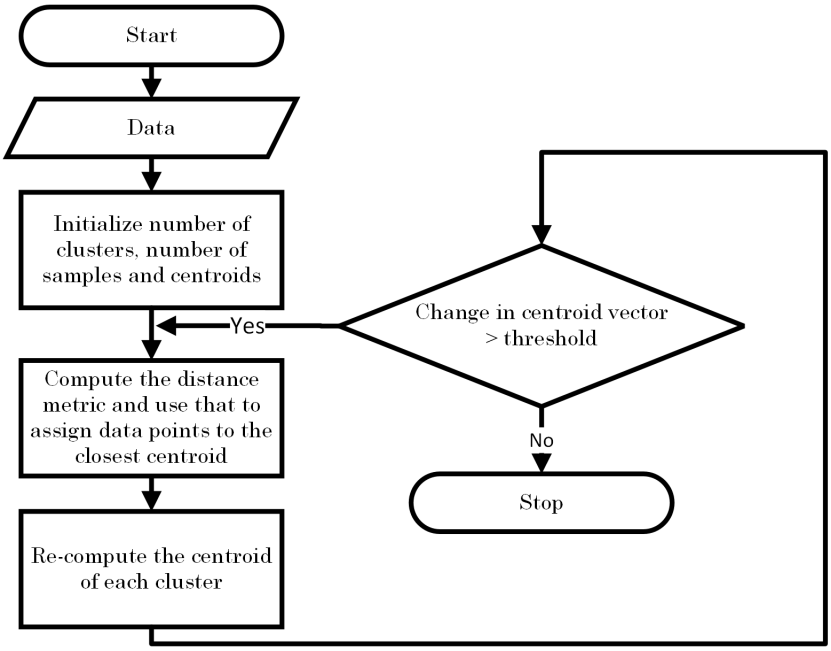

Fig. 2 K-means clustering algorithm flowchart

UAVs, we implemented k-means clustering on relevant features obtained from the UAV sensors that are directly or indirectly related to vibrations, either as cause or effect. The exact features considered in this paper have been explored from UAV flight test data as described in section IV.B.2. In this section we define the general approach of k-means clustering [17].

k-means clustering is a simple unsupervised classification method that uses a distance metric for clustering. It classifies feature data into k different clusters (user defined) based on their signatures. Since UAV flight data for vibration studies lack classification labels, k-means method provides insight into if the flight data can be grouped together based on vibration related features and their correlation. This method clusters data points by minimizing the intra-cluster distance, i.e. distance between data points in a cluster, while maximizing the inter-cluster distance, i.e. distance between clusters. After initializing the number of clusters k and the cluster centroids, data samples are clustered with their nearest centroid using a distance metric. Many different metrics can be used, but here we used Mahalanobis distance [18]). After that, the centroid is redefined by computing the mean of all new data points assigned to that cluster. Cluster assignment and centroid re-computation continues until the change in centroid vectors drop below a threshold and there is no further change in cluster assignment of the data sets. Figure 2 illustrates a simple flowchart of k-means clustering method. Although k-means clustering method is simple and effective, proper choice of the number of clusters, initialization, and distance metric are critical for its performance. To optimize k, we calculated the average distances of all data points to their respective cluster's centroid for a range of values (e.g., for 1 to 10) for k, then select the value for k with the least average intra-cluster distance. This ensures the optimum number of clusters with the highest cluster tightness or separability.

IV. Vibration analysis on data from UAV flight experiments

In this paper, two different sets of UAV flight experiment data were studied for analysis of vibration characteristics in presence of wind. Observations from each of these datasets are reported in this section.

A. NASA Langley Research Center UAV flight data

The data for this study was collected at NASA Langley Research Center (LaRC) [1] under four flight tests using an octocopter in autonomous mode, equipped with Pixhawk hardware and controlled with Ardupilot software. Figure 3(b) shows the aircraft used for this study.

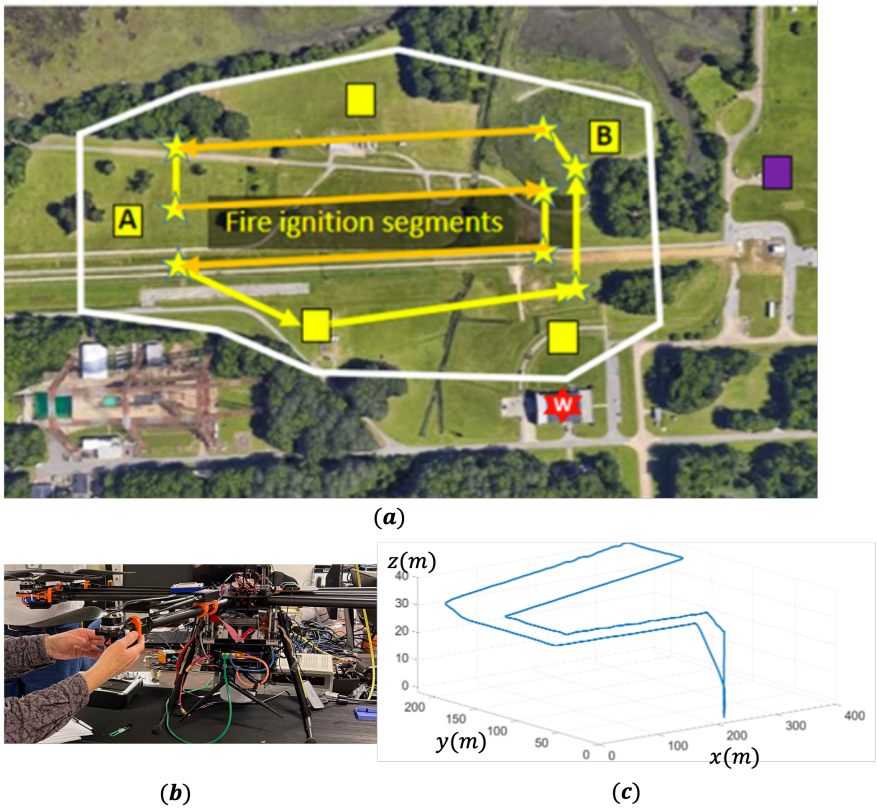

(*a*) (*b*) (*c*)

Fig. 3 (a) Flight plan at NASA Langley Research Center (b) Tarot octocopter installed with Ardupilot vibrational sensors (c) Flight trajectory followed by a UAV in x-y-z coordinates.

Data collected by the aircraft included aircraft status, such as power drawn, position, and heading information, IMU data from an accelerometer and gyroscope, and vibration data. All data obtained from the aircraft was sampled at a rate of $2Hz$. We note that these sensors were located at the center of the aircraft, and sensor data for the individual motors was not available. All four test flights followed the same flight plan as shown in Figure 3(a) where the trajectory followed by the UAV consisted of 9 waypoints as shown in Figure 3(c).

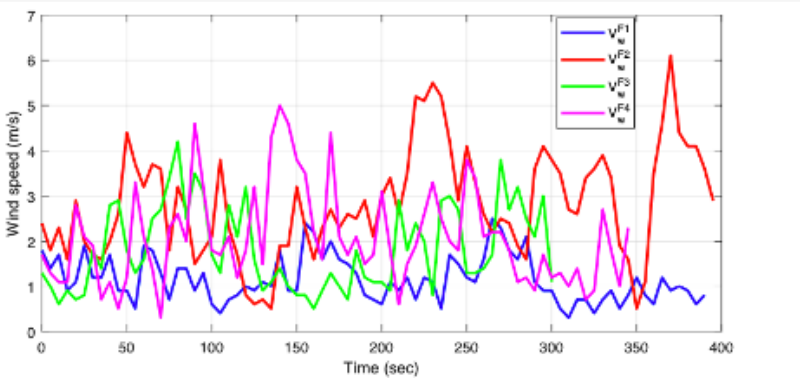

Fig. 4 Wind data recorded for flights F1- F4.

The flights had the following UAV ground speed and wind speed profiles:

- Flt 41: low ground speed ($5m/s$) with mostly low wind speeds ($< 2.5m/s$)
- Flt 43: low ground speed ($5m/s$) with mostly high wind speeds ($< 6m/s$)

- Flt 44: high ground speed ($8m/s$) with mostly high wind speeds ($< 5m/s$)
- Flt 45: high and low ground speeds ($8m/s$ and $3m/s$ during final segment of flight) with mostly high wind speeds ($< 4.5m/s$)

Wind speed data was collected by a Centralized PI Controller located within $100m$ of the flight path and was sampled once every $5s$. The location of the wind sensor is denoted as the red star in Figure 3 (a). This data further included the heading of the wind, without any knowledge of the wind's vertical component. The effect of surrounding trees and buildings is not considered for this analysis. The wind speed data for the four flights is plotted in Figure 4.

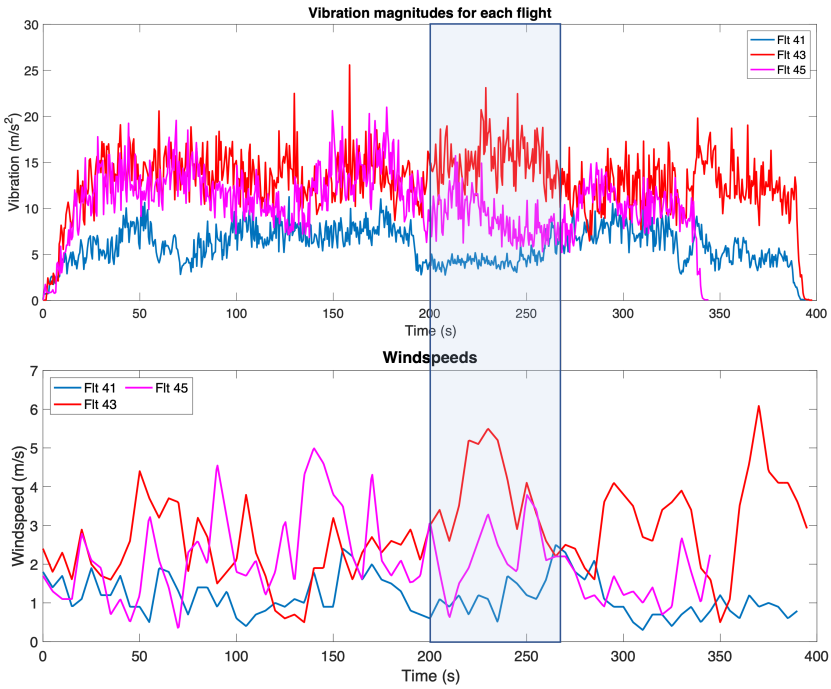

Fig. 5 (a) Vibration magnitudes (b) Corresponding wind profiles for flights F1 (Flt 41), F2 (Flt 43) and F4 (Flt 45).

The vibration data was collected for the x, y, and z axes of the aircraft, where the x and y axes are parallel to the body of the aircraft and the x axis points toward the front of the aircraft; the z axis represents the vertical component. As previously mentioned, this data was collected at a rate of 2 Hz. Collection began a few minutes prior to flight and concluded about a minute after flight. The data was trimmed to only include the time window of interest. This time frame was determined based on when the z axis acceleration showing significant increase, indicating take off, and concluded when these values stopped changing, indicating landing.

1. Initial Observations from Vibration Measurements

The vibration magnitudes computed from the three axes for flights F1, F2 and F4 are shown in Figure 5. The corresponding histograms of the vibration data along the three separate axis are shown in Figure 6. From these Figures, it can be deduced that wind magnitude has an effect on the overall vibration magnitude, i.e. with higher winds, the UAV recorded higher vibration levels. The variance in the vibration measurements stays the same for all wind conditions, which is assumed to be more of a characterization of the sensor itself irrespective of the wind it encounters.

The other important observation from these flight experiments is that vibrations encountered by a UAV depends on its air speed in addition to the wind speed. Figure 7 shows the corresponding ground speed profile for the four flights, as measured by the on-board navigation sensors. Figure 7(a) compares flights F1 and F2 whereas Figure 7(b) compares flights F3 and F4. The highlighted section of Figure 7(a) indicates higher vibration levels for high wind scenario, given both flights have the same UAV ground speed profile. On the other hand, in Figure 7(b), the highlighted section indicates that for similar wind speed, vibrations recorded by a UAV flying at a higher speed is higher compared to a low-speed UAV. The reason could be that a UAV flying at a higher speed demands higher rotor speed and if there is a propeller

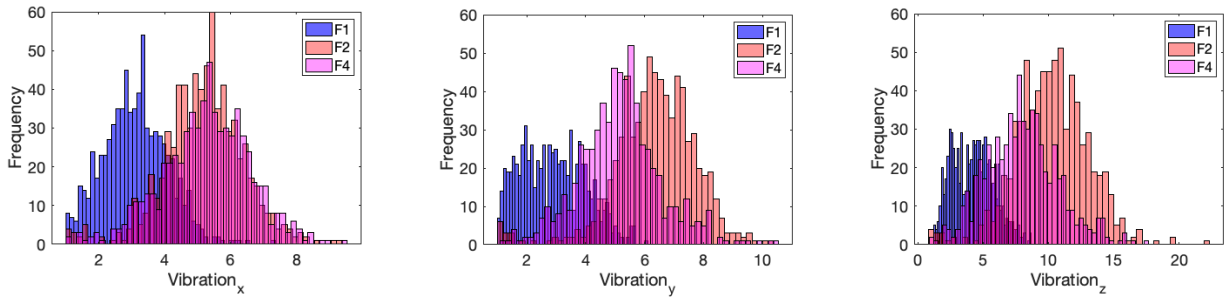

Fig. 6 Histogram of vibration data for Flight F1, F2, and F3 along the (a) x-axis, (b) y-axis and (c) z-axis.

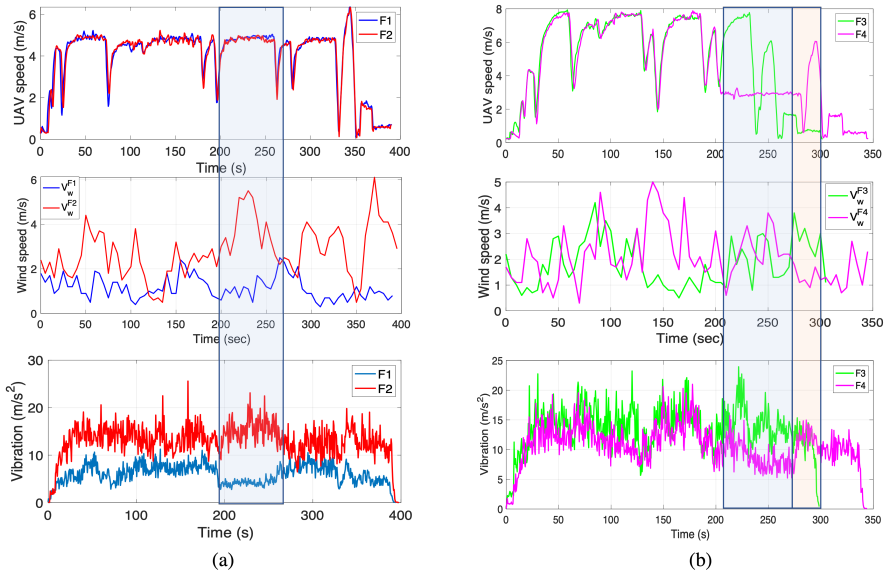

Fig. 7 Vibrations corresponding to UAV ground speed and wind speed for (a) Flights F1 and F2 and (b) Flights F3 and F4.

imbalance or the vehicle frame imbalance, overall vibrations become more pronounced, compared to a low-speed UAV.

B. University of Notre Dame UAV flight data

The second set of data that was analysed for this paper was obtained from UAV flight experiments conducted at the University of Notre Dame with Streamline Design HX10 drones equipped with their DroneResponse onboard autonomous pilot software [19, 20]. The autonomous pilot was built using Python and MavROS. Data was collected from a total of 16 flights, comprising different trajectories such as circles, zigzags, and straight paths and conducted at different wind conditions. The wind was characterized by GFS27 wind forecasts at a location $10m$ from to the flight path with information on the wind speed magnitude, direction and wind gust.

1. Initial Observations from Vibration Measurements

For the first analysis, flights 1 and 3 were compared, where the UAV flew a triangular trajectory as shown in Figure 8, with Figure 8(a) showing the map of the flight path in the university of Notre Dame flight zone and Figure 8 (b) depicting the post-flight GPS measurements plotted in latitude-longitude coordinates.

The corresponding wind measurements for these two flights acquired at the beginning of each of the flights are mentioned in the Table 2.

Data obtained from the on-board vibration sensor is plotted for the two flights in Figure 9. As can be seen in Figure

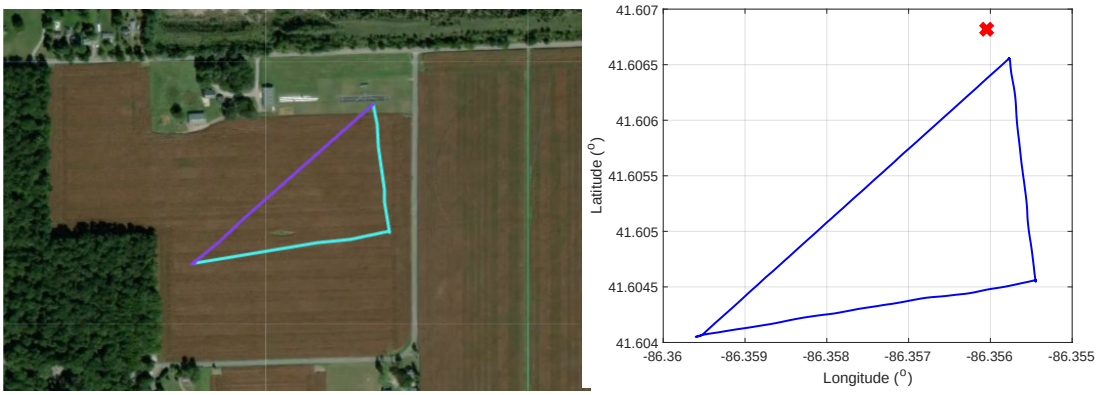

(a) (b)

Fig. 8 UAV flight plan at University of Notre Dame for flights F1 and F3 (a) on map (b) plot with red cross denoting location of wind measurements.

Table 2 Wind characteristics from GFS27 forecast model for flights F1 and F3.

	Wind speed Magnitude	Wind speed Direction	Wind Gust
F1	8.26 kts	SW	N/A
F3	5.4 kts	SW	10 kts

9, flight F3 had a strong wind gust recorded at $10kts$ and had a median vibration of $7.75m/s^2$, in comparison to flight F1 where no or minimal wind gust was encountered which had median vibration of $3.94m/s^2$.

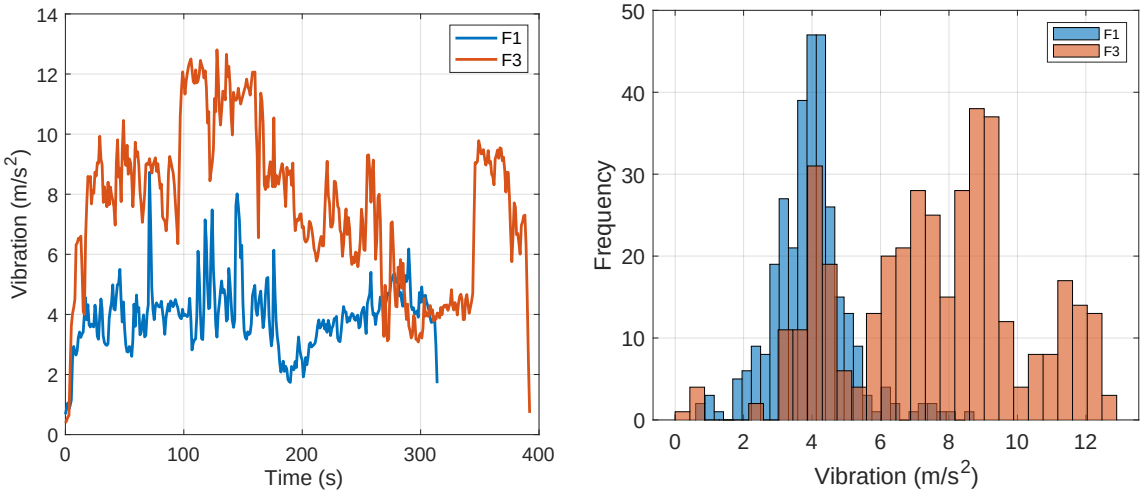

(a) (b)

Fig. 9 (a)Vibration signals for flights F1 and F3 (b) Corresponding histograms.

Two other flights, F12 and F16, comprised of the same straight-path flight trajectory with the experiments being conducted at different wind conditions were compared with analogous methods. The wind characteristics of these two flights are recorded in Table 3.

Table 3 Wind characteristics from GFS27 forecast model for flights F12 and F16.

	Wind Speed Magnitude	Wind Speed Direction	Wind Gust
F12	8 kts	SE	11 kts
F16	12 kts	SE	17.5 kts

For flights F12 and F16, the UAV followed the same trajectory under same wind direction (SE), but the magnitude of wind speed and wind gusts differed, as seen from Table 3. It should be noted that flight 16 had to be terminated early (at 65 s), due to wind gusts being higher than its safe limit, but we still use its data for analysis in order to study the effect of wind on vibration recorded by the UAV. The trajectory of these flights along with the corresponding vibration signals are plotted in Figure 10. Comparing the vibration magnitude plots and histogram indicates that for higher wind speed magnitude and higher wind gusts, the UAV encounters stronger vibration under similar flight plan and same wind direction. Even though data from Flight 16 was limited due to early termination of the flight, the median of its vibration magnitude (flown at wind gust of $17.5kts$) is at $7.05m/s^2$, almost double of that for flight 12 (flown at wind gust of $11kts$) whose median vibration value was at $4.15m/s^2$.

Although we had a single wind measurement and could not comment on the temporal variation of the wind along the entire flight trajectory for this dataset, the vibration amplitude can be seen to be increasing with higher wind gusts. Additionally, the effect of UAV flight heading and its relation to the wind direction would be investigated in future studies.

2. k-means clustering on the vibration data

The clustering algorithm was implemented on the Notre Dame flight dataset since we had access to data for numerous flights, along with the corresponding wind gust values and UAV component related parameters such as the propeller imbalance metric. We did not have similar parameters from the NASA LaRC data and hence skipped the clustering analysis on that dataset for this study. We intend to investigate other vibration related parameters from the LaRC dataset in the future and demonstrate clustering analysis on those.

From each of the 16 flight tests in Notre Dame dataset, features with high correlation with the vibration signal were extracted and considered for the clustering analysis. As understood from the FMEA and initial observations from the two flight test dataset, high vibration seems to have correlation with wind gust magnitude, UAV airspeed, and any vehicle propeller blade information. With that observation, features specific to vibration, wind, UAV speed, and imbalance propeller metric (additional data recorded by UAV autopilot in the Notre Dame dataset) were prepared, as defined in the following steps:

1) Obtain the trimmed time-series vibration signal from the UAV on-board sensor, as shown in Figure 11 (b). This signal is acquired at a data rate of 1 Hz in the Notre Dame dataset.
2) Plot the histogram of the time-series signal as shown in Figure 11 (a).
3) Identify the bins with highest frequency of vibration data. Record the edges of these top 5 bins, shown in Figure 11 (b). This 5-array data is recorded as the vibration magnitude features for each flight.
4) Identify the 5 timestamps when the UAV records the 5 peak vibration magnitudes.
5) Record the 5 values of UAV speed (given by on-board GPS data) and imbalance propeller metric at the 5 timestamps corresponding to peak vibrations, shown in Figure 11 (b). These are recorded as features related to UAV speed and imbalance propeller metric for each flight.
6) Record the wind gust value for the particular flight. Since there is no temporal information of the wind in this dataset, we resort to defining a 5-vector array of constant wind gust value for all the 5 points. This is the wind gust feature.
7) Repeat for all flights. Each flight will therefore be described by 5 points, each with four dimensions: $\{Vibration-magnitude, Wind-gust, Imbalance-propeller-metric, UAV-speed\}$

It should be noted that instead of selecting highest peaks from the vibration signal, we selected highest occurrence values as the relevant features for clustering. This is because, sudden peaks in the time-series of vibration signal may originate due to multiple reasons including change in attitude, change in acceleration at trajectory turns or even sensor noise. These may be biased depending on the trajectory and may not accurately represent a vibration anomaly caused by wind gusts or propeller imbalance. Higher occurrence values from the vibration histogram ensured the selection of

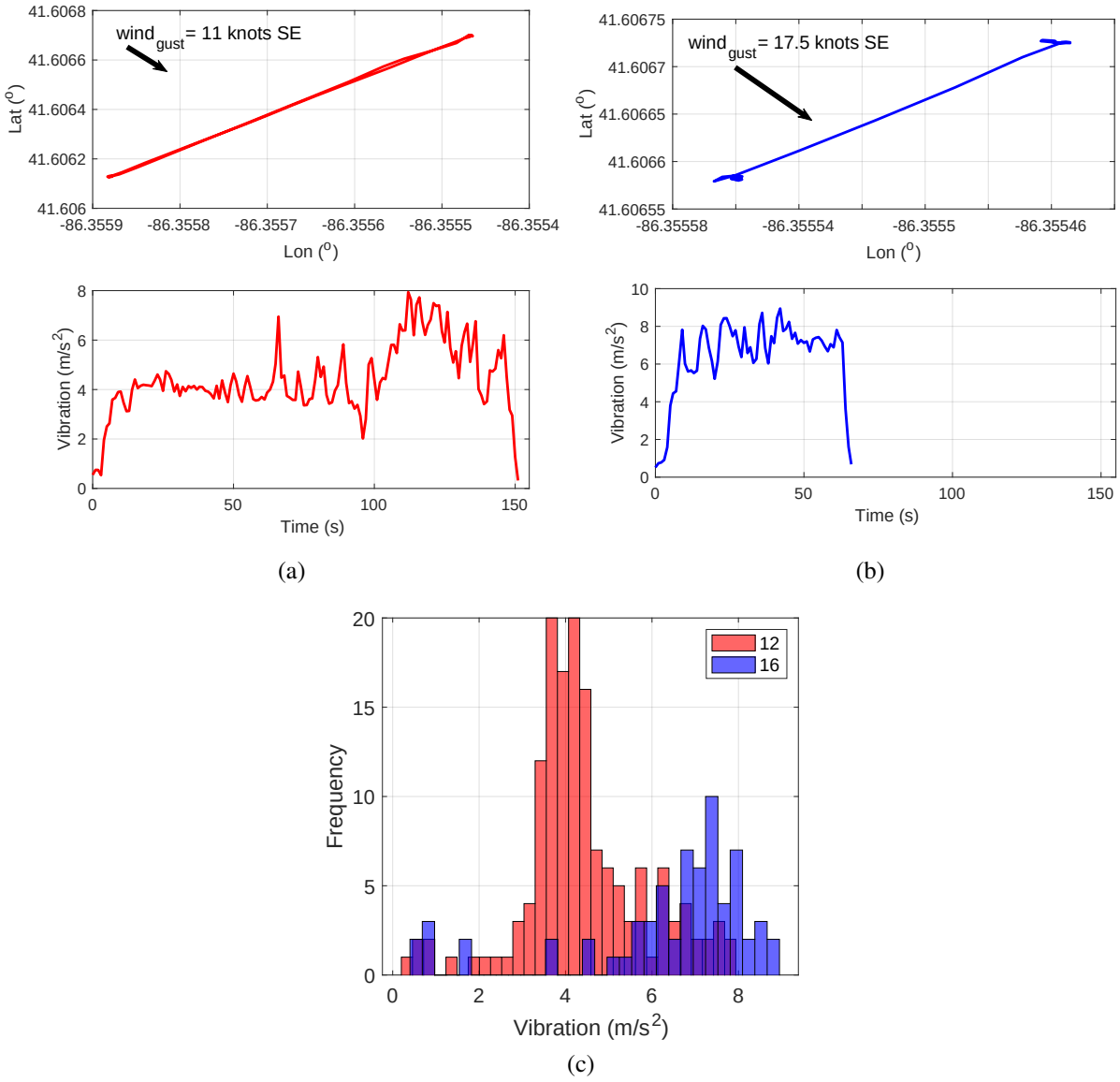

Fig. 10 (a)Flight trajectory and vibration signals for flight F12 (b)Flight trajectory and vibration signals for flight F16 and (c) histogram of corresponding vibration signals.

sustained feature points throughout the entire flight and performed better in clustering with higher separation between clusters.

Out of the 16 flight data, F2, F8, and F15 were discarded as they consisted of either incomplete or incorrect flight logs. From the remaining 13 flights, 10 were used for training the k-means clustering algorithm to determine the optimum number of clusters and the cluster centroids, whereas the other three were the test data assigned to specific clusters based on the nearest centroid. The clusters were generated from the training data set using the three dimensions $\{Vibration-magnitude, Wind-gust, Imbalance-propeller-metric\}$ as shown in Figure 12. $UAV-speed$ did not prove to be a distinguishing feature in this dataset, and hence is not shown in these results. Additionally, for many of the flights, NaN values were recorded under the $Imbalance-propeller-metric$. For such flights, the specific feature was replaced with zero to still be able to use this flight data in our analysis.

As can be observed, minimizing the average intra-cluster distance yielded an optimal number of clusters of $k = 4$. The our distinct clusters are denoted by the four colors in Figure 12. The red markers correspond to the flights $F9$ and

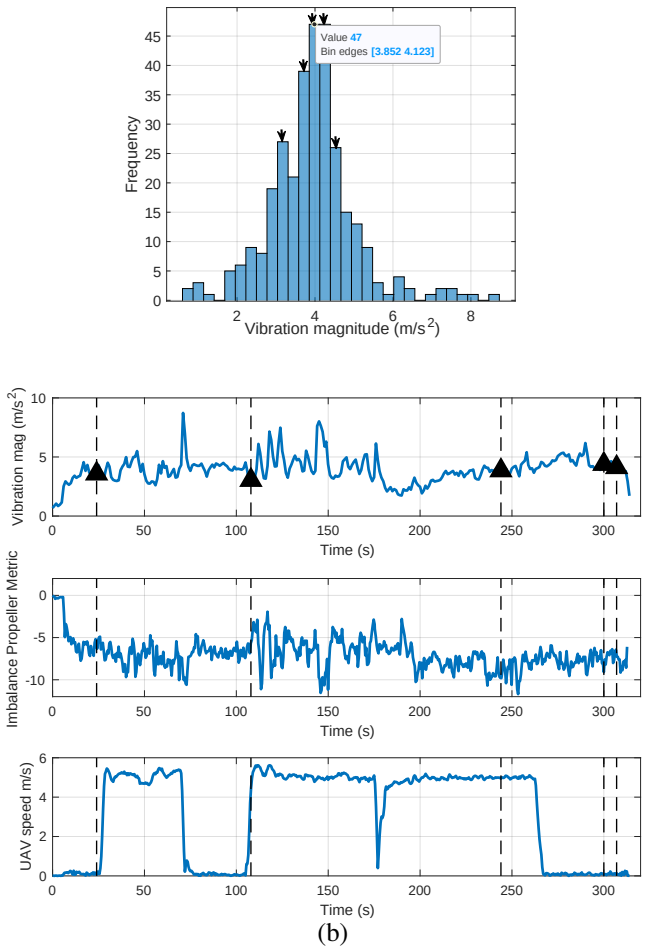

(b)

Fig. 11 Feature extraction from the three signals recorded in UAV flight F1. (a) Vibration magnitude histogram with top five bins (b) Features from all signals at the same timestamp corresponding to top five bin edges.

$F10$ which recorded the least vibration in its on-board sensor. The propeller imbalance metric was a value close to zero or NaN for these flights, indicating minimal imbalance in their propellers or no information. This cluster may be assumed to originate from nominal vibration levels, given low vibration magnitude.

The green cluster is from flights F5, F14 and F16. These flights recorded high wind gusts (greater than $14kts$) during their flight times, and encountered higher vibration levels. The blue cluster corresponds to flights F4, F6, F7, and F12 where these flights flew at medium wind gust levels ranging from $9-11kts$ and hence they recorded lower vibration compared to green cluster points. Finally, the magenta points are of particular interest. They originate from flight F1, which corresponded to a less windy day and hence recorded vibration levels lower than the blue and green clusters, but higher than the nominal feature points marked in red. Additionally, F1 also recorded high propeller imbalance metric and formed its own distinct cluster, as shown in Figure 12. On further post-flight analysis, it was found that the UAV in F1 was under-powered compared to its weight and its actuator outputs were fluctuating greatly with frequent minimum and maximum clippings indicating heavy and imbalanced payload and anomalous vibrations. This was an indication that our approach was able to determine this as a cluster of its own and separate from the nominal flights (red markers). Overall, the four colored clusters can be assumed to have the following meaning and health index attached to them, as stated in Table 4.

The test data features from flights F3, F11, and F13 were assigned to the respective clusters by the k-means algorithm, based on its least Mahalanobis distance from the cluster centroids. These are marked by stars and their respective assigned clusters are denoted with the corresponding cluster colors in Figure. 12. The features of flight F11 overlap

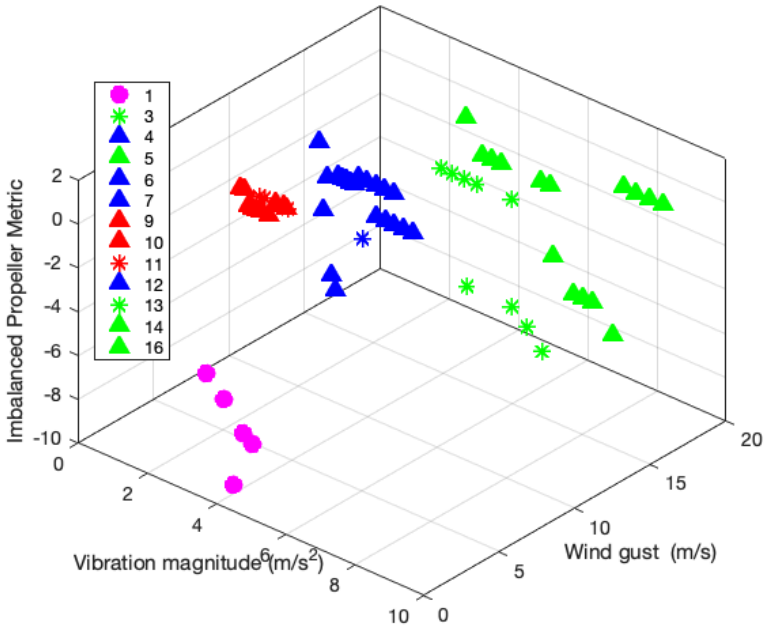

Fig. 12 Results from k-means ($k = 4$) clustering analysis on the UAV Notre Dame data: star markers denote the test data features and remaining are from training data.

Table 4 Clustering analysis results.

Cluster color	Vibration	Wind Gust	Propeller Imbalance	Health Index
Red	Low	Low-Moderate	Low	NOMINAL
Blue	Low-Moderate	Moderate-High	Moderate	OFF-NOMINAL
Green	High	High	Moderate	OFF-NOMINAL
Magenta	Low-Moderate	Low	High	OFF-NOMINAL

with the red cluster and was assigned as the nominal flight with low vibrations. Flight F13 recorded high vibrations and faced higher wind gusts and was hence assigned to the green cluster. On the other hand, for flight F3, one out of five of its feature points was assigned to the blue cluster based on its closest distance to the centroid. However, since the other four feature points were assigned to the green cluster, the overall F3 data point ended up in the "high-wind, high vibration –> OFF-NOMINAL" label.

V. Conclusion

In this paper, effect of wind on vibrations encountered in UAVs have been discussed. Criticality of vibration monitoring in flights have been established through thorough review of related literature and different sources of vibration relation failures have been identified. With that understanding, signals affecting vibrations have been investigated in data from UAV flight experiments conducted at two locations. Further, nominal and off-nominal categories of flight data were obtained via k-means clustering of features extracted from the on-board sensor outputs. Vibration magnitude, wind gust and imbalanced propeller measures have been useful in determining the clusters. In the future, other related parameters of interest related to UAV vibrations such as wind speed direction, UAV attitudes, UAV battery SOC drop and IMU sensor faults will be investigated. The clustering approach will be extended to more flight data and the assignment results on test data flights will be validated in post-flight analysis.

Acknowledgment

This work was supported by the System-Wide Safety (SWS) project under the Airspace Operations and Safety Program within the NASA Aeronautics Research Mission Directorate (ARMD). The authors thank Kyle Smalling and

Patrick Quach from NASA Langley Research Center, for managing the UAV flight experiments, as well as Chris Morris from Safety Critical Avionics Systems Branch for managing the ground sensor based CEPIC wind data and making it available for research use. The authors would also thank Jane Huang and Walter Scheirer from University of Notre Dame for leading the UAV flight experiments conducted at Notre Dame under NSF award number:1931962 and sharing the data for analysis.

References

[1] Young, S. D., Ancel, E., Dill, E. T., Moore, A., Quach, C. C., Smalling, K. M., and Ellis, K. K., "Flight Testing In-Time Safety Assurance Technologies for UAS Operations," *AIAA Aviation 2022 Forum*, 2022, p. 3458.

[2] Palanisamy, R. P., Kulkarni, C. S., Corbetta, M., and Banerjee, P., "Fault detection and Performance Monitoring of Propellers in Electric UAV," *2022 IEEE Aerospace Conference (AERO)*, IEEE, 2022, pp. 1–6.

[3] Ghimire, R., Corbetta, M., and Palanisamy, R. P., "Fault Detection and Diagnosis Techniques for Electric UAV Powertrain System," *2023 IEEE Aerospace Conference (AERO)*, IEEE, 2022, pp. x–x.

[4] Al-Badour, F., Sunar, M., and Cheded, L., "Vibration analysis of rotating machinery using time–frequency analysis and wavelet techniques," *Mechanical Systems and Signal Processing*, Vol. 25, No. 6, 2011, pp. 2083–2101.

[5] Bektash, O., and la Cour-Harbo, A., "Vibration analysis for anomaly detection in unmanned aircraft," *ANNUAL CONFERENCE OF THE PROGNOSTICS AND HEALTH MANAGEMENT SOCIETY 2020*, PHM Society, 2020.

[6] Banerjee, P., Okolo, W. A., and Moore, A. J., "In-flight detection of vibration anomalies in unmanned aerial vehicles," *Journal of Nondestructive Evaluation, Diagnostics and Prognostics of Engineering Systems*, Vol. 3, No. 4, 2020.

[7] Bondyra, A., Gasior, P., Gardecki, S., and Kasiński, A., "Fault diagnosis and condition monitoring of UAV rotor using signal processing," *2017 Signal Processing: Algorithms, Architectures, Arrangements, and Applications (SPA)*, IEEE, 2017, pp. 233–238.

[8] Verbeke, J., and Debruyne, S., "Vibration analysis of a UAV multirotor frame," *Proceedings of isma 2016 international conference on noise and vibration engineering*, 2016, pp. 2401–2409.

[9] Feng, Z., Liang, M., and Chu, F., "Recent advances in time–frequency analysis methods for machinery fault diagnosis: A review with application examples," *Mechanical Systems and Signal Processing*, Vol. 38, No. 1, 2013, pp. 165–205.

[10] Neild, S., McFadden, P., and Williams, M., "A review of time-frequency methods for structural vibration analysis," *Engineering Structures*, Vol. 25, No. 6, 2003, pp. 713–728.

[11] Romberg, T., Cassar, A., and Harris, R., "A comparison of traditional Fourier and maximum entropy spectral methods for vibration analysis," 1984.

[12] Banerjee, P., Corbetta, M., and Jarvis, K., "Probability of Obstacle Collision for UAVs in presence of Wind," *AIAA AVIATION 2022 Forum*, 2022, p. 3460.

[13] Wang, B. H., Wang, D. B., Ali, Z. A., Ting, B. T., and Wang, H., "An overview of various kinds of wind effects on unmanned aerial vehicle," *Measurement and Control*, Vol. 52, No. 7-8, 2019, pp. 731–739. https://doi.org/10.1177/0020294019847688, URL https://doi.org/10.1177/0020294019847688.

[14] Ge, C., Dunno, K., Singh, M. A., Yuan, L., and Lu, L.-X., "Development of a Drone's Vibration, Shock, and Atmospheric Profiles," *Applied Sciences*, Vol. 11, No. 11, 2021. URL https://www.mdpi.com/2076-3417/11/11/5176.

[15] Kulkarni, C. S., Corbetta, M., and Robinson, E. I., "Systems Health Monitoring: Integrating FMEA into Bayesian Networks," *2021 IEEE Aerospace Conference (50100)*, 2021, pp. 1–11. https://doi.org/10.1109/AERO50100.2021.9438219.

[16] Freeman, P. M., "Reliability assessment for low-cost unmanned aerial vehicles," Ph.D. thesis, University of Minnesota, 2014.

[17] Duda, R. O., Hart, P. E., et al., *Pattern classification*, John Wiley & Sons, 2006.

[18] Melnykov, I., and Melnykov, V., "On K-means algorithm with the use of Mahalanobis distances," *Statistics & Probability Letters*, Vol. 84, 2014, pp. 88–95.

[19] Al Islam, M. N., Chowdhury, M. T., Huang, J. C., and Spirkovska, L., "Towards an Annotated All-Weather Dataset of Flight Logs for Small Uncrewed Aerial Systems," *AIAA AVIATION 2023 Forum*, 2023.

[20] Al Islam, M. N., Chowdhury, M. T., Agrawal, A., Murphy, M., Mehta, R., Kudriavtseva, D., Cleland-Huang, J., Vierhauser, M., and Chechik, M., "Configuring mission-specific behavior in a product line of collaborating Small Unmanned Aerial Systems," *Journal of Systems and Software*, Vol. 197, 2023, p. 111543.